Appendix 5C-3: Evaluation of Phosphorus Sources, Forms, Flux, and Transformation Processes in the Stormwater Treatment Areas

INTRODUCTION

The overarching goal of the phosphorus (P) flux study is to enhance the understanding of the mechanisms and factors that affect P treatment performance of stormwater treatment areas (STAs), particularly those that are key performance drivers at the lower reaches of the treatment trains. In order to understand the mechanisms and factors that affect STA performance at low total phosphorus (TP) concentrations, it is imperative to evaluate the P sources, forms, flux, and transformation processes along the STA flow-ways. A better understanding of the mechanisms and factors that affect P treatment performance of the STAs at low TP concentrations is vital to develop strategies that could improve capabilities of the STAs to achieve permit compliance with water quality based effluent limits (WQBELs). The P flux study was designed to address two key Restoration Strategies Science Plan questions:

- How can internal loading of P to the water column be reduced or controlled, especially in the lower reaches of the treatment trains?
- How can the biogeochemical or physical mechanisms be managed to further reduce soluble reactive phosphorus (SRP), particulate phosphorus (PP), and dissolved organic phosphorus (DOP) concentrations in the outflow of the STAs?

The P flux study consists of several substudies designed to collectively address the two key questions, and they include (1) data mining, (2) organic P speciation, (3) flow-way assessments at different flow conditions, (4) in situ particle dynamics, (5) in situ P flux measurements, (6) soil characterization, (7) assessment of enzyme and microbial activity, (8) vegetation assessments, and (9) quantification of faunal role in P cycling. In addition, limited data will be collected at Water Conservation Area 2A (WCA-2A) for comparison purposes. These substudies are in various stages of implementation. Preliminary results from the following four substudies are presented in this appendix:

- Evaluation of Historical Surface Water, Porewater, and Soil Data Collected within Selected Flow-Ways
- Flow-Way Water Quality Assessments
- Phosphorus Flux Measurements
- Effects of Faunal Communities on the Water Quality in the Everglades Stormwater Treatment Areas

Several terms pertaining to P cycling appear throughout this section and are defined as follows:

- ***Flux*:** movement or exchange of P between two compartments or matrices (e.g., soil and surface water). The term "flux" is directionless and does not imply movement into or out of any particular compartment.
- ***Diffusive flux*:** movement of dissolved constituents between soil/porewater and the surface water, as driven by unequal concentrations. According to the laws of diffusion, this flux moves dissolved molecules from regions of higher concentrations to regions of lower concentrations, but otherwise implies no particular direction of movement.
- ***Flux potential*:** the negative of the slope of porewater P concentrations measured across the -4 to +4 centimeter (cm) soil-water interface (based on porewater equilibrator data). Positive flux potential values indicate an upward P gradient between soil porewater and the lower water column, and negative values indicate a downward gradient between soil porewater and the lower water column.
- ***Net flux*:** the combined (net) movement of P into or out of the surface water, including all potential interacting compartments or matrices, such as soil, porewater, algae, or macrophytes. Processes contributing to net flux may include diffusive flux, resuspension, and decomposition. The term "net flux" is directionless, but reflects results in the surface water column.

EVALUATION OF HISTORICAL SURFACE WATER, POREWATER, AND SOIL DATA COLLECTED WITHIN SELECTED FLOW-WAYS

John Juston[1]

INTRODUCTION AND METHODS

To complement the many new and diverse data collections in the P flux study, additional data mining was conducted based on data from different STA flow-ways collected from 2005 to 2010. Primarily, this effort was to determine trends and relationships among P-related variables in STA soils, porewater, and surface water, particularly in the lower reaches of the treatment flow-way. Analysis was completed across a pooled database and within individual flow-way data sets.

The assembled database represented 86 separate sites from sampling events along standardized internal grids in STA-2 Cells 1, 2, and 3; STA-3/4 Flow-way 2; and STA-5 Flow-way 2. The strength of this collective database is that measurements were conducted at co-located sites, although not all variables were measured at all sites or in all data sets. Data were analyzed using bivariate correlation analysis and multivariate principal component analysis (PCA). Bivariate correlations were developed for two data treatments: (1) the complete pooled data set (n = 86), and (2) a low-P data subset representing typically back-end STA locations with water TP levels of less than 20 micrograms per liter (µg/L) at the time of soil and porewater sampling (n = 25).

[1] Juston Hydro AB, Stockholm, Sweden

RESULTS

Key results indicated that a chain of significant correlations exists between soil P, porewater P, and water column P concentrations, even in the subset of data that represented only low-P conditions. Based on the strength of correlations, soil TP appeared to be an acceptable indicator of P flux potential from STA soils, but the data suggest that the labile P fraction derived using sodium bicarbonate ($NaHCO_3$)-extraction (i.e., Olsen-P) (Olsen et al. 1954) is a better indicator. The potential for P flux appeared to exhibit breakpoint-type behavior with Olsen-P and soil TP concentration levels. Specifically, low or no P gradients were evident at low soil P concentrations (< 60 milligrams per kilogram [mg/kg] Olsen-P; < 800 mg/kg soil TP); above these thresholds, elevated and increasing vertical gradients were observed. Finally, some non-P porewater variables that were hypothesized to influence P flux had no apparent relationships (e.g., redox potential), while others were correlated (e.g., ammonium [NH_4^+], pH). These relationships should be further investigated using the new data collected from the P flux study before drawing strong conclusions. Results from PCA support an assessment of cohesion of P-related variables across soil, porewater, and water column matrices. Taken together, these results support and help refine the South Florida Water Management District's (SFWMD's or District's) conceptual P cycle models, and should be useful to help guide the current P flux study.

Complete methods and results are reported in DB Environmental, Inc. (DBE 2016b). Selected key results are presented in further detail below. Bivariate relationships were grouped sequentially by (1) P and non-P porewater variables, (2) soils and porewater P variables, and (3) porewater and water column P variables. These results are followed by the multi-variate PCA.

Porewater Variable Correlations

Table 1 shows a correlation matrix that focuses on interrelationships between measured porewater variables only. Results are shown symbolically, in the table index; the symbols also pertain to subsequent tables. Results indicate that all non-P variables were significantly correlated with one another, either positively or negatively, in the full and low-P database sets (**Table 1**). For example, alkalinity shows a strong positive correlation to dissolved calcium concentrations and is negatively correlated with redox potential.

Positive correlations exist between all the measured porewater P variables, including SRP and DOP concentrations and calculated SRP and DOP flux potentials (**Table 1**). Flux potentials were defined as the negative of the slope of porewater P concentrations measured across the -4 to +4 cm soil-water interface (based on porewater equilibrator data). Positive flux potential values indicate an upward P gradient between soil porewater and the lower water column. For example, as expected, there was a strong positive correlation between SRP concentrations and flux potentials. This occurs as elevated porewater concentrations create higher concentration differentials across the soil-water interface, thus driving the potential for diffusive fluxes. As an example of how some of these relationships appear in cross-plots, **Figure 1** shows calculated SRP flux potential values versus measured SRP concentrations (0–4 cm average) for all available data and for the low-P subset. **Figure 2** shows similar trends for DOP and DOP flux potentials, which were strongly correlated within both data sets. In the low-P domain, the potential for flux from soils to the water-column were almost the same for SRP and DOP species (compare ranges in **Figures 1** and **2**).

The correlation results in **Table 1** suggest that the only significant relationships crossing between P and non-P porewater variables were with ammonium and pH levels. Other variables, including redox potential, had no correlation with porewater P concentrations or flux potentials across both data sets. The lack of correlation with redox, which is contrary to what was expected in a wetland system, will be investigated further.

Table 1. Symbolic correlation matrix showing results for porewater variables only. The matrix is symmetric about the diagonal, such that columns and corresponding rows show the same results. Heavy interior lines group non-P and P variables.

		Porewater, 0-4 cm								
		Alk	**NH_4**	**Ca**	**Eh**	**pH**	**SRP**	**DOP**	**SRP_{flux_pot}**	**DOP_{flux_pot}**
Porewater, 0-4 cm	Alkalinity	1	++	++	--	0-				
	Ammonium	++	1	++	--	--	++	+	+	++
	Calcium	++	++	1	-	--				
	Eh (Redox)	--	--	-	1	0+				
	pH	0-	--	--	0+	1	-		-	--
	SRP		++			-	1	++	++	++
	DOP		+			0	++	1	+	++
	SRP_{flux_pot}		+			-	++	+	1	+
	DOP_{flux_pot}		++			--	++	++	+	1

Index of Symbols Used

blank	no significant relationship
+	significant positive Spearman ranked correlation coefficient (r_s) across all data sets
+	significant correlation has $r_s > 0.7$
-	significant negative correlations across all data sets
++	significant positive correlations in both the full pooled database and in the low-P database subset
++	significant correlations in both the full and low-P data; the correlation in low-P subset has $r_s > 0.7$
++	highly significant correlations in both the full and low-P data ($r_s > 0.7$)
0+; 0-	significant positive or negative correlations in the low-P subset only.

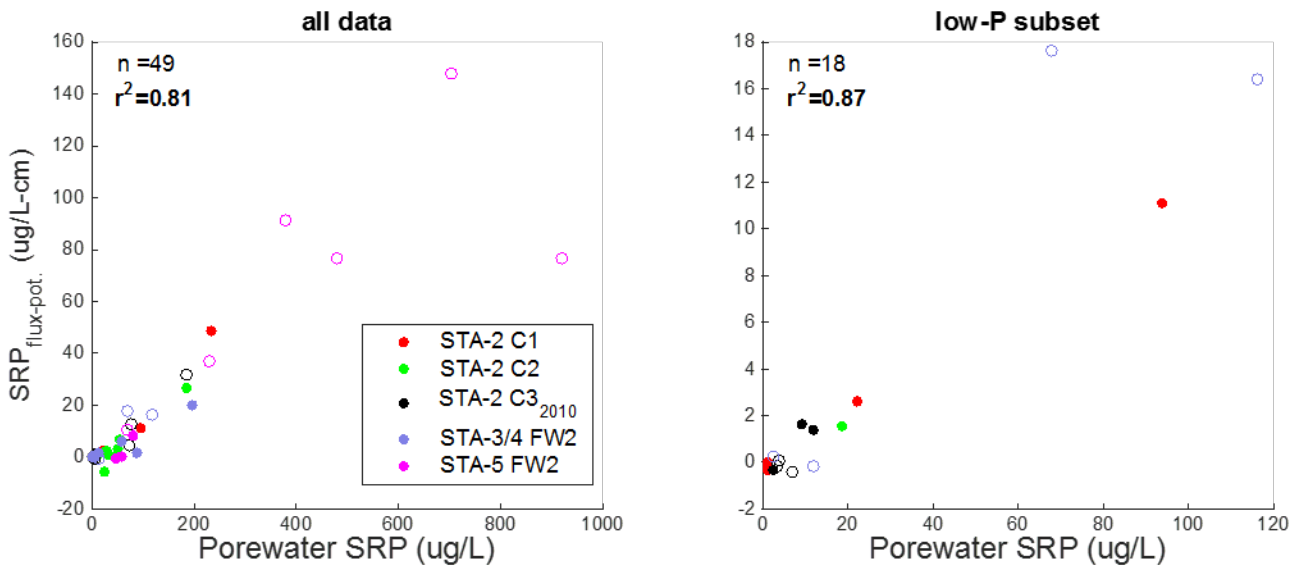

Figure 1. Cross-plots of porewater SRP concentrations and SRP flux potentials based on all data and the low-P data set (defined as those from sites with surface water TP < 20 µg/L at the time of soil and porewater sampling). Dots are color-coded by flow-way, as shown in the legend. Open dot symbols indicate submerged aquatic vegetation (SAV)-dominated sites, closed dots indicate emergent aquatic vegetation (EAV)-dominated sites. Net sample sizes are noted in the upper left of each plot; not all data sets contained all data variables. X and Y axis scales are different in each plot.

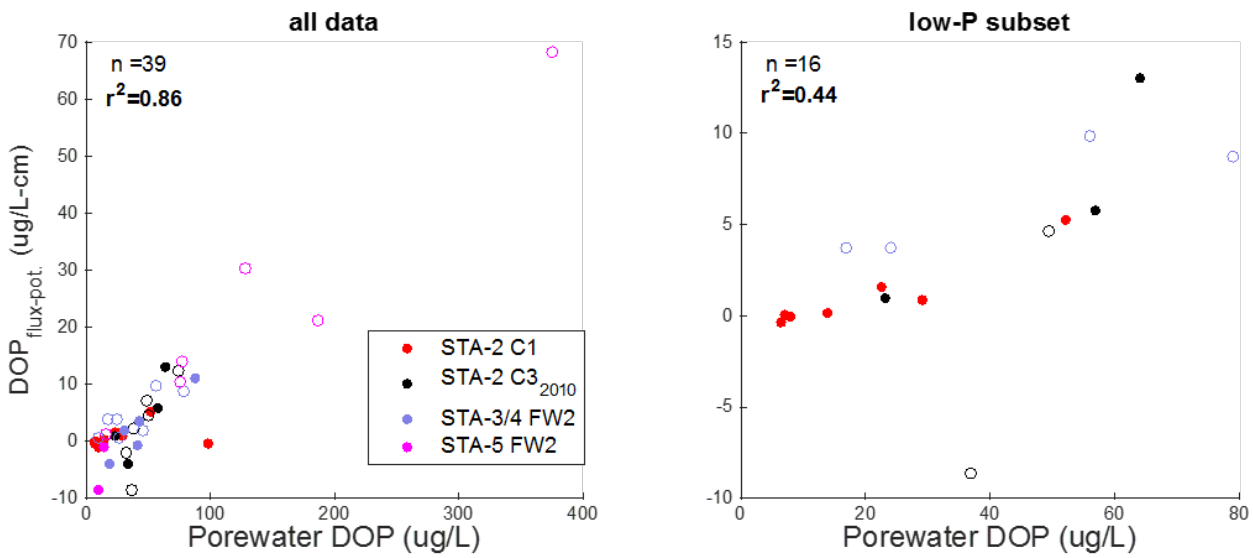

Figure 2. Cross-plots of porewater DOP concentrations and calculated DOP flux potentials.

Soils and Porewater Phosphorus Variable Correlations

Table 2 shows a symbolic correlation matrix that focuses on interrelationships between bulk soil properties and porewater P data variables. The four non-P variables were strongly correlated to one another based on the complete database and the low-P data subset. For example, soil total carbon showed a strong positive correlation to total nitrogen (TN) concentrations, and was inversely related to soil total calcium levels. Relationships among soil P variables generally were not as strong or consistent as the non-P variables. For example, soil TP was weakly correlated to Olsen-P levels, but only when all available data are considered and not in the low-P subset.

Table 2. Symbolic correlation matrix for soils and porewater variables. Symbols are the same as those defined in **Table 1**. Heavy interior lines delineate soils and porewater variables. Not all variable pairs were available for calculating correlation statistics (shown with 'NaN').

		Soil Properties, 0-4 cm								Porewater			
		TC	TOC	TCa	TN	TP	Olsen-P	Labile-P	Semi +lab	SRP	DOP	SRP_{flux_pot}	DOP_{flux_pot}
Soil properties, 0-4 cm	TC	1	++	--	++	+	-	NaN	NaN				
	TOC	++	1	--	++	+	-	NaN	NaN				
	TCa	--	--	1	--	-	+	NaN	NaN				
	TN	++	++	--	1	+	-	NaN	NaN				
	TP	+	+	-	+	1	+	+	++	+		+	
	Olsen-P	-	-	+	-	+	1	+		++	+	++	0+
	Labile-P	NaN	NaN	NaN	NaN	+	+	1	+				
	Semi+Lab P	NaN	NaN	NaN	NaN	++		+	1	0-			0-
Porewater	SRP					+	++		0-	1	++	++	++
	DOP						+			++	1	+	++
	SRP_{flux_pot}					+	++			++	+	1	+
	DOP_{flux_pot}						0+		0-	++	++	+	1

The results in **Table 2** suggest that the only significant relationships crossing between soil and porewater P variables were through soil TP, Olsen-P, and the sum of labile and semi-labile P (in low-P regions only) variables. Non-P soil variables were not correlated with porewater P variables (**Table 2**), or non-P porewater variables for that matter.

Soil Olsen-P appears to be a more consistent and sensitive indicator of SRP and DOP flux potentials than soil TP (**Table 2**). Olsen-P values were significantly correlated to porewater SRP concentrations and flux potentials based on all available data and on the low-P data subset, and correlated to DOP flux potentials at low-P sites. On the other hand, at low-P sites, soil TP concentrations were not correlated to porewater SRP variables or to DOP variables (**Table 2**).

Figures 3 and **4** show cross-plots of SRP flux potential versus soil TP and Olsen-P values to support the finding described in the previous paragraph. Visual examination of these plots indicates a possible breakpoint or threshold behavior of flux potentials and STA soils P concentrations. This is particularly evident in the relationships with Olsen-P (**Figure 5**), which show flattened, near-zero flux potentials below 60 mg/kg Olsen-P, and a tendency toward elevated values with greater variance above that. Data from three different data sets contribute values above and below this apparent breakpoint. These observations are

furthered in **Figure 6**, which plots porewater SRP profiles lumped into two categories of Olsen-P, above and below 60 mg/kg. Here again, low porewater SRP concentrations and flattened profiles (i.e., low flux potentials) are consistently found and clearly demonstrated at sites with low Olsen-P concentrations. For soil TP, a possible breakpoint appears at about 800 mg/kg (**Figure 3**); however there are still many sites with soil TP greater than 800 mg/kg with low flux potentials. **Figure 6** shows a supporting plot of all available porewater SRP profiles (n = 49) grouped into three different categories of soil-TP: below 800 mg/kg, above 1,500 mg/kg, and in between.

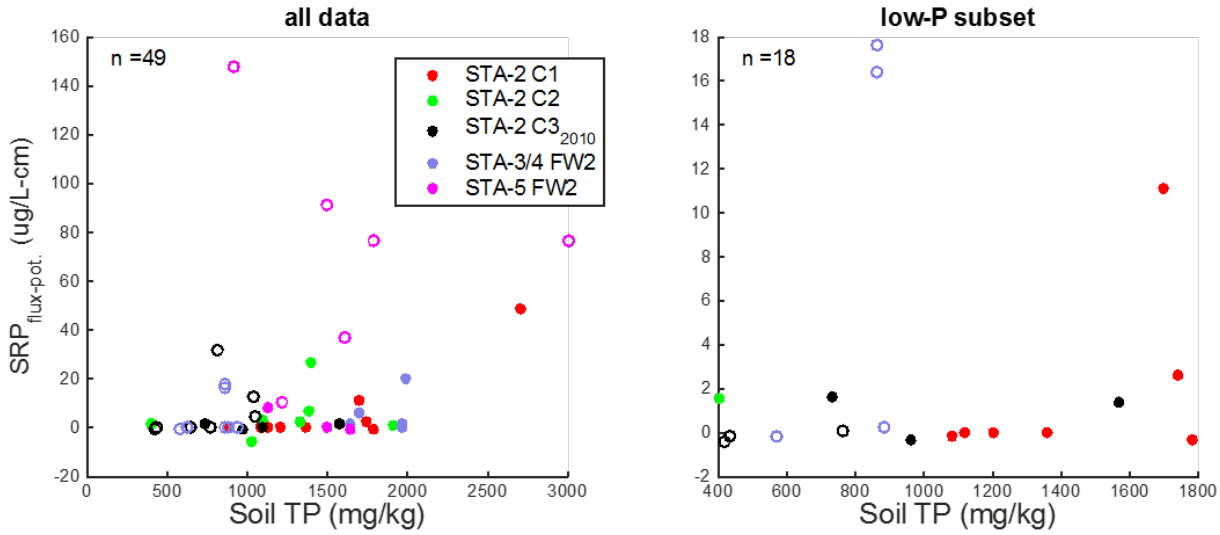

Figure 3. Cross-plots of soil TP concentrations and calculated SRP flux potentials.

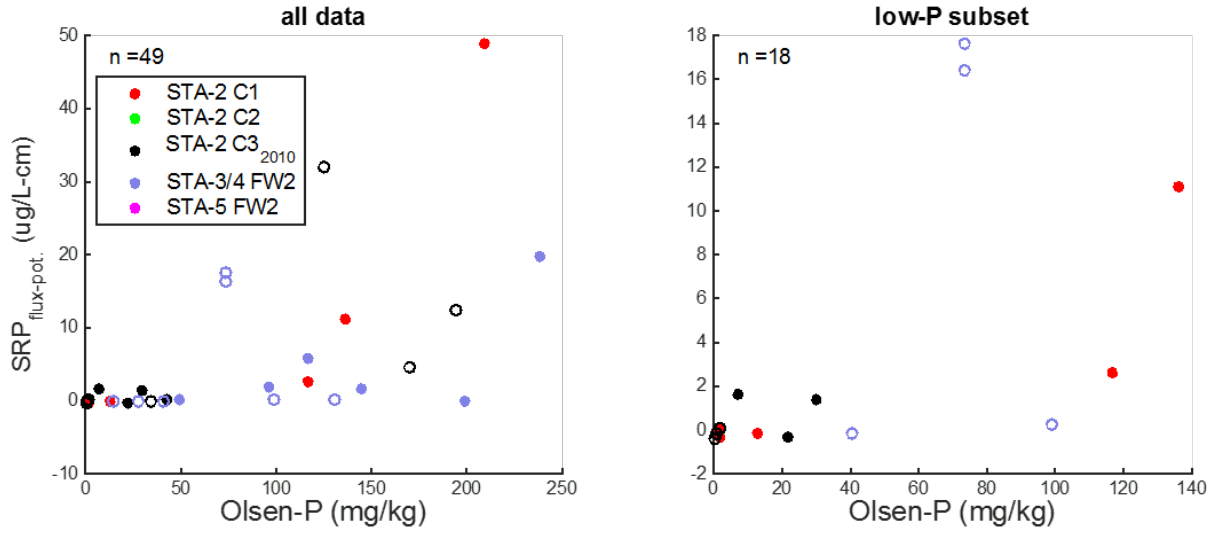

Figure 4. Cross-plots of soil Olsen-P concentrations and calculated SRP flux potentials.

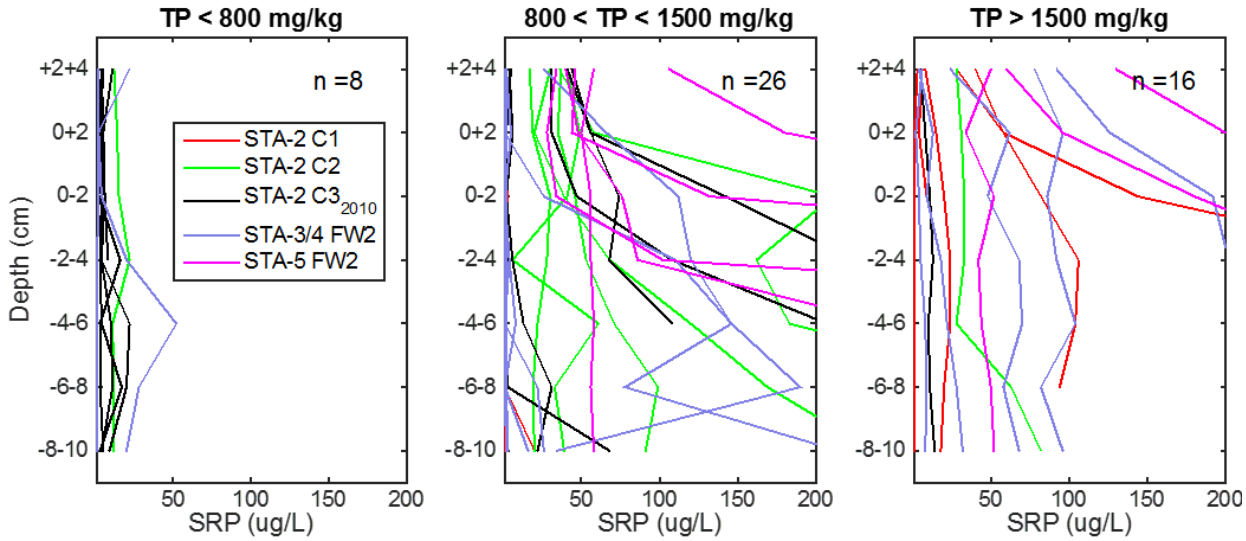

Figure 5. Available porewater SRP profiles classified by magnitude of soil TP. Data from STA-5 Flowway 2 was available and included, which was performing poorly during this time.

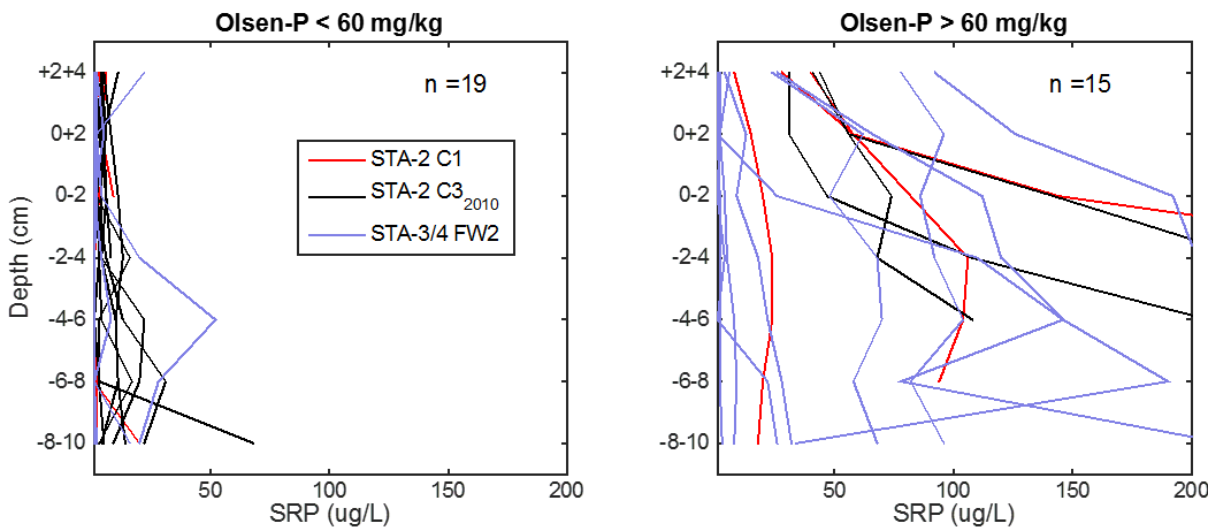

Figure 6. All available porewater SRP profiles classified by magnitude of soil Olsen-P. Olsen-P groupings were determined by visual assessment. The three available data sets in this plot represent three well-performing STAs.

Surface and Porewater Phosphorus Variable Correlations

The previous two subsections identified correlations that connect soil P properties to porewater P concentrations and porewater P concentrations to flux potentials in the STAs. The following analysis was performed to determine the relationship between porewater flux potentials and surface water P concentrations (**Table 3**).

Significant correlations exist between surface water SRP concentrations and porewater SRP flux potentials based on all available data and the low-P subset (**Table 3**). **Figure 7** shows cross-plots of these data relationships. In the low-P subset, all surface water SRP concentrations were below 4 µg/L, yet a significant relationship still exists between the extreme low values and independently measured porewater

SRP concentrations and flux potentials. Also, note that within the surface water P variables, PP was the P fraction with strongest and most consistent correlation to TP concentrations based on the full pooled STA data set and low-P subset.

Table 3. Symbolic correlation matrix for surface- and porewater variables. Results among the four porewater P variables are the same as shown in **Table 1**.

		Surface water				Porewater, 0-4 cm			
		SRP	DOP	PP	TP	SRP	DOP	SRP_{flux_pot}	DOP_{flux_pot}
Surface	SRP	1	+	+	+	+	+	++	
	DOP	+	1	+	+	+		+	
	PP	+	+	1	++	+		0+	
	TP	+	+	++	1	++	0+	++	
Porewater	SRP	+	+	+	++	1	++	++	++
	DOP	+			0+	++	1	+	++
	SRP_{flux_pot}	++	+	0+	++	++	+	1	+
	DOP_{flux_pot}					++	++	+	1

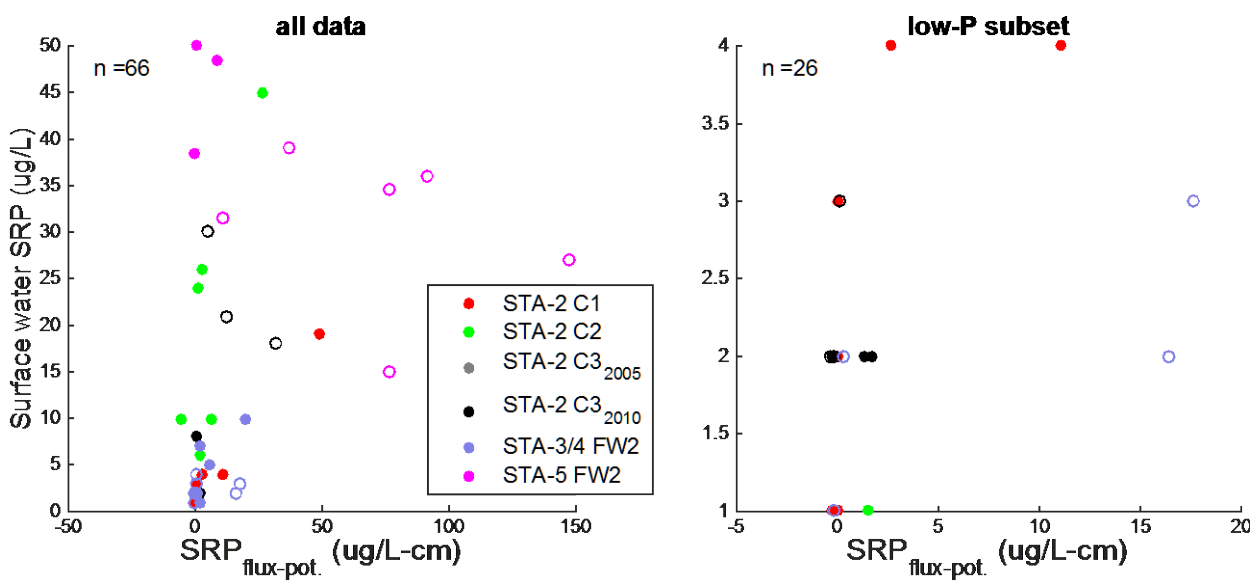

Figure 7. Cross-plots of porewater SRP flux potential and surface water SRP concentrations. (Note that visual inspection, which is most akin to a Pearson-type assessment of correlation, of the low-P subset does not strongly suggest an existing correlation; however, significant Spearman rank correlations were identified [**Table 3**]).

Principal Component Analysis

PCA was used to explore the structure of the data sets for internal STA measurements (conducted within the interior of the flow-ways). Due to wide differences in data dimensionality, data variables were standardized (z-scale transformation) to avoid misclassification prior to PCA. Bi-plots representing results of PCA are shown in **Figure 8**. Bi-plots are graphical tools used to represent the first two or three principal components from PCA. The plots show the first two components from two data subset screenings (31 sites representing 11 data variables, and 29 sites representing 15 data variables), where the dominant component in each was rotated to align with the x-axis. Data variables are shown as vectors in bi-plots, where vector orientation indicates the extent to which the variance in those variables was captured by component 1 or 2. In general, the two components explain a sufficient amount of the variance to provide a meaningful visual representation of the structure of variables in the two database subsets (68 and 60 percent, respectively). Three-dimensional plots quickly become difficult to interpret.

In both PCAs, the available non-P variables align mostly along the first principal component direction, and P variables align essentially orthogonally with the second component (excepting $DOP_{flux\ pot}$ in PCA2, which is intermediate). Thus, data values for P-related variables in soil (Olsen-P), porewater (SRP and DOP concentrations, SRP flux potential), surface water concentrations (TP, SRP, and DOP), and incubation studies (14-day SRP release) tend to cluster together in regards to covariance, while variability in non-P related porewater variables was largely independent (i.e., orthogonal), but with strong interrelationships to one another. The PCA results provide strong support for the findings of the bivariate correlation analyses in the preceding section.

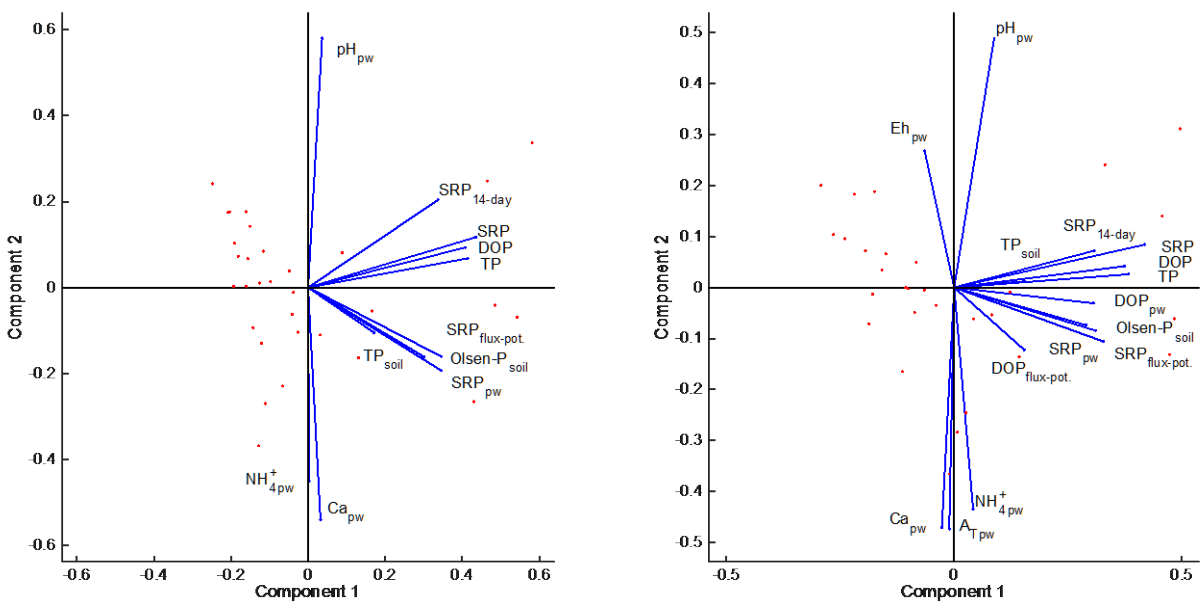

Figure 8. PCA results for PCA1 and PCA2 data subsets. The two data eigenvectors illustrated in each panel described 68 and 60 percent of the total variance in the source data sets, respectively.

FLOW-WAY WATER QUALITY ASSESSMENTS

Odi Villapando, Rupesh Bhomia[2], Jill King, and Paul Julian[2]

INTRODUCTION

This field study is an evaluation of the biogeochemical responses of the different regions along the selected STA flow-ways to three different flow scenarios: stagnant, low flow, and high flow. These flow tests will provide quantitative and qualitative information on nutrient dynamics in the water column under different flow scenarios that will be used to determine the factors influencing the measured biogeochemical responses and their relative magnitudes, particularly those related to P sources, P flux, and P species transformations.

METHODS

The STA flow-ways chosen for this study were STA-2 Cell 1, STA-2 Cell 3, and STA-3/4 Cells 3A and 3B. These specific flow-ways were selected to represent good performing flow-ways (those that have achieved outflow TP concentration of 13 µg/L or lower) versus less effective flow-ways (those that have achieved outflow TP concentration between 13 and 30 µg/L), and represent different cell configurations, vegetation communities, and soil conditions. Three flow events have been completed so far, two in STA-2 Cell 1 and one in STA-2 Cell 3. The results presented here are from the last flow event conducted in Cell 3 of STA-2 (**Figure 9**). This is a single cell flow-way with predominantly submerged aquatic vegetation (SAV) and a large patch of emergent aquatic vegetation (EAV) in the eastern region of the cell. The native soil in the cell is highly organic but the current soil in the STA has inorganic floc deposited over the organic soil layer. The annual outflow flow-weighted mean TP concentration for this cell is 17 µg/L.

The flow event in STA-2 Cell 3 was conducted from February 22 to April 11, 2016. This event consisted of a "high flow" (average 325 cubic feet per second [cfs]) period from February 22 to March 6, 2016, followed by a stagnant (no inflow) period from March 7 to 28, 2016, and then a post-stagnation operational period from March 29 to April 11, 2016. (**Figure 10**). The post-stagnation operational flows were defined as inflows to the cell that occur in response to upstream basin runoff. During the post-stagnant operational period, the cell received an average flow of 51 cfs.

Continuous monitoring of water quality and field conditions during the flow event was conducted at six water quality monitoring stations installed along the middle transect of the treatment flow-way (**Figure 9**). The stations were equipped with autosamplers, EXO-sondes, water level loggers, and HOBO light meters. The autosamplers collected water samples every 4 hours (2 am, 6 am, 10 am, 2 pm, 6 pm, and 10 pm), which were analyzed for TP on discrete samples and TN and total organic carbon (TOC) on daily composited samples. Weekly surface grab samples were also collected from these sites and analyzed for TP, SRP, total dissolved P (TDP), dissolved organic carbon (DOC), TN, calcium (Ca), magnesium (Mg), potassium (K), sodium (Na), ammonium, nitrogen oxides (NO_x), iron (Fe), sulfate (SO_4^{2-}), chloride (Cl), alkalinity, color, total suspended solids (TSS), hardness, and chlorophyll. In situ measurements of pH, temperature, specific conductivity, and dissolved oxygen at 15-minute intervals were collected using EXO-sondes. PP was calculated as the difference between TP and TDP, and DOP was calculated as the difference between TDP and SRP. The following section focuses on autosampler TP data and P forms from weekly grab sampling and other selected water quality parameters.

[2] Wetland Biogeochemistry Laboratory, University of Florida, Gainesville, FL

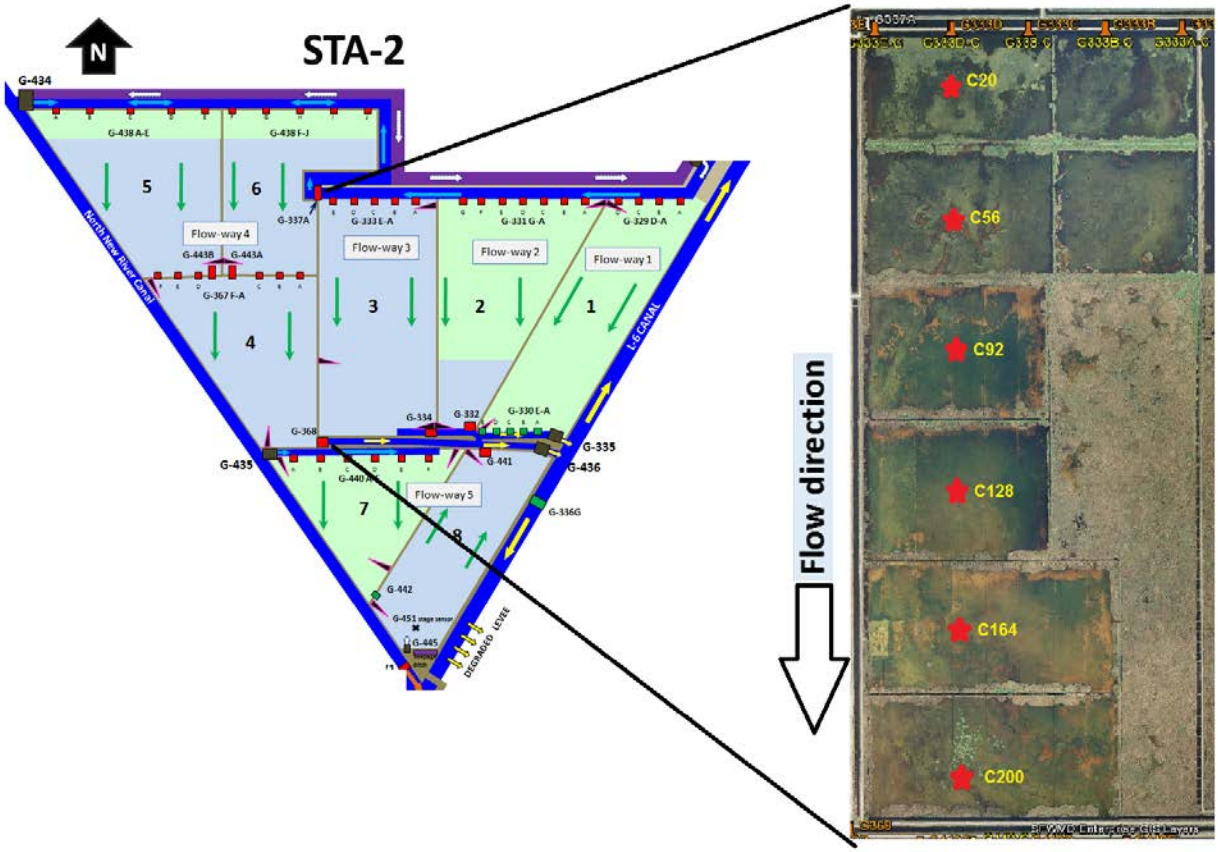

Figure 9. STA-2 Cell 3 map showing the water quality monitoring stations.

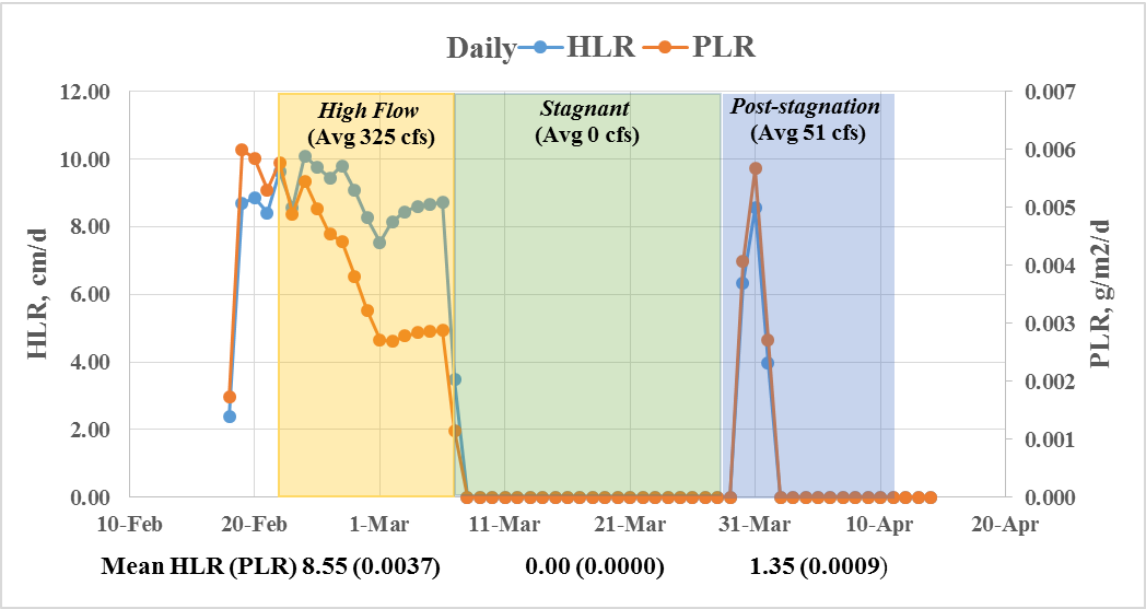

Figure 10. Hydrologic conditions during the flow event. HLR is hydraulic loading rate in centimeters per day (cm/d) and PLR is phosphorus loading rate in grams per square meter per day (g m^2/d).

RESULTS

Autosampler Total Phosphorus Concentrations

Autosampler TP data were screened for outliers using a non-parametric approach, in which values greater than the 99th percentile for a given station and flow period were identified as an outlier and removed from further statistical analysis (Julian and Hill 2012). Overall, 893 samples were collected with 31 of these identified as outliers. Almost 50 percent of the outliers (15 out of 31) came from Station C56 under stagnant condition where wildlife activity documented on March 18–22, 2016 could have compromised sample integrity.

There was a clear TP concentration gradient along the treatment flow-way at all phases of the flow event (**Figure 11**). Water column TP concentrations at all stations were lowest during the high-flow period and highest under stagnant condition. The occurrence of the high TP concentrations observed under stagnant conditions will be investigated further in additional flow scenarios and in concert with other substudies that are being implemented as part of the P flux study. TP concentrations at all stations following the stagnant phase exhibited a decreasing trend. TP concentration at Station C20 was unusually high due to high-velocity flows that came through the cell during the first three days of post-stagnation period (**Figure 10**). Differences in TP concentrations for all stations across flow events were significantly different at a significance level of $\alpha = 0.05$ using Kruskal-Wallis Rank Sum Test ($\chi^2 = 163.70$, DF = 5, $p < 0.05$) (**Figure 12**). While the spatial pattern in TP concentrations along the treatment flow-way demonstrates distinct reduction, the spike in TP concentration at Station C92 particularly under stagnant condition suggests localized internal P loading. An evaluation of the soils, vegetation, and microbial data collected along the transect will be conducted to provide plausible explanations for P release/reduction mechanisms operating within this region of the cell.

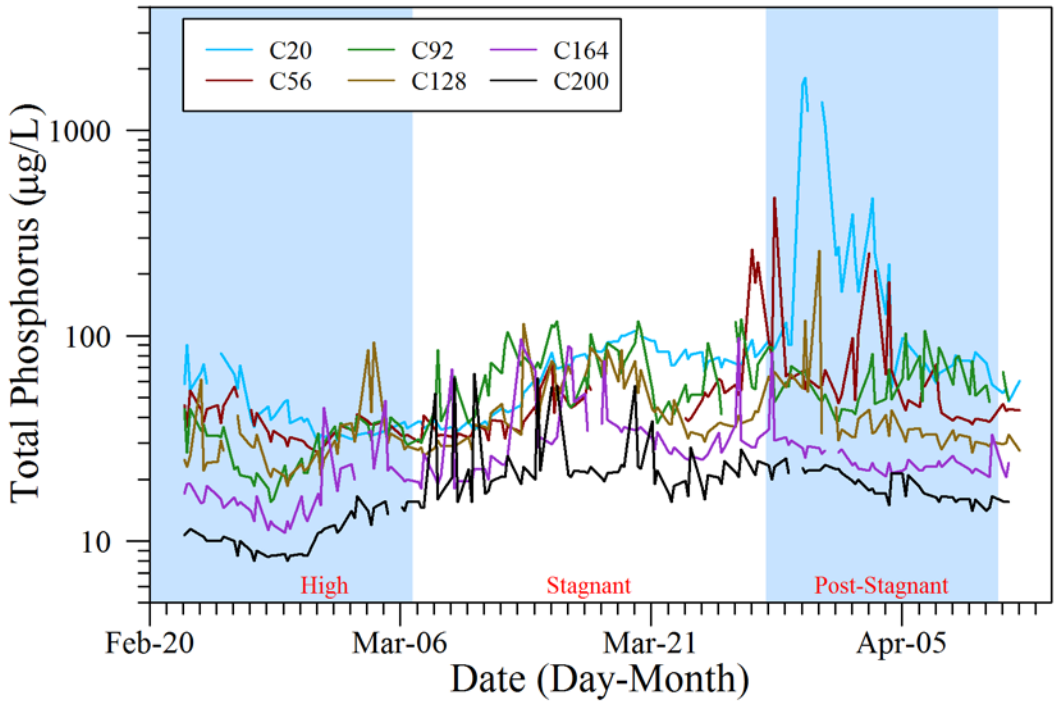

Figure 11. Autosampler TP concentrations at the different locations along the treatment flow-way for the entire flow event. Note y-axis is on a log-scale and outliers were removed.

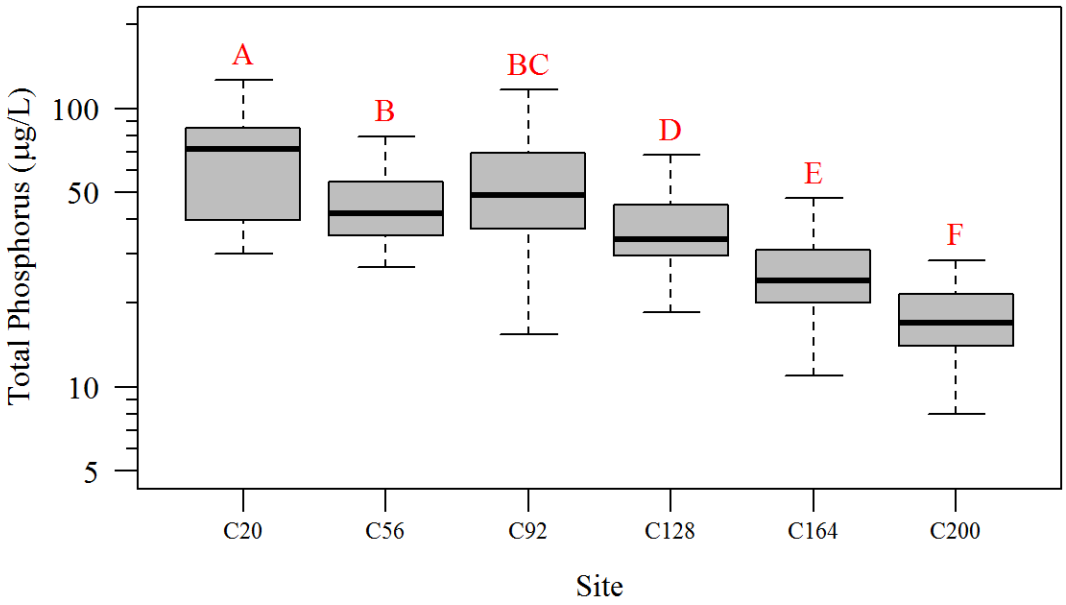

Figure 12. Boxplot of 4-hour TP data for all stations across flow periods. Mean TP concentrations for any two stations with the same letter are not significantly different at α = 0.05 using Dunn's test of multiple comparisons. Note y-axis is on a log-scale.

Weekly Grab Water Column Phosphorus Concentrations and Forms

The changes in P forms and concentrations along the treatment path during the flow event were monitored in weekly grab samples. Consistent with autosampler TP, the weekly grab TP showed P reduction at all phases of the flow event (**Figure 13**). Mean outflow TP concentrations were 12, 24, and 15 µg/L at the end of high, stagnant, and post-stagnant operational flow periods, respectively, for an average reduction in concentration of approximately 20 percent. The majority of the reduction in TP is due to reduction in PP, which accounted for 32 to 73 percent of TP. Both DOP and SRP were reduced gradually along the flow-way; SRP reduction was more consistent and greater than that for DOP. SRP reached minimum detection limit (2 µg/L) starting at the mid-region of the cell (Station C128) during the entire flow event, indicating that this P fraction was consumed much more quickly by biotic and abiotic components of the wetland as the water traveled down the flow-way. Similar to autosampler TP, the grab TP concentrations were elevated following the high-flow event and during the stagnant period, but started to decline upon resumption of post-stagnation operational period. The release of P under stagnant conditions has important implications for STA operations and performance.

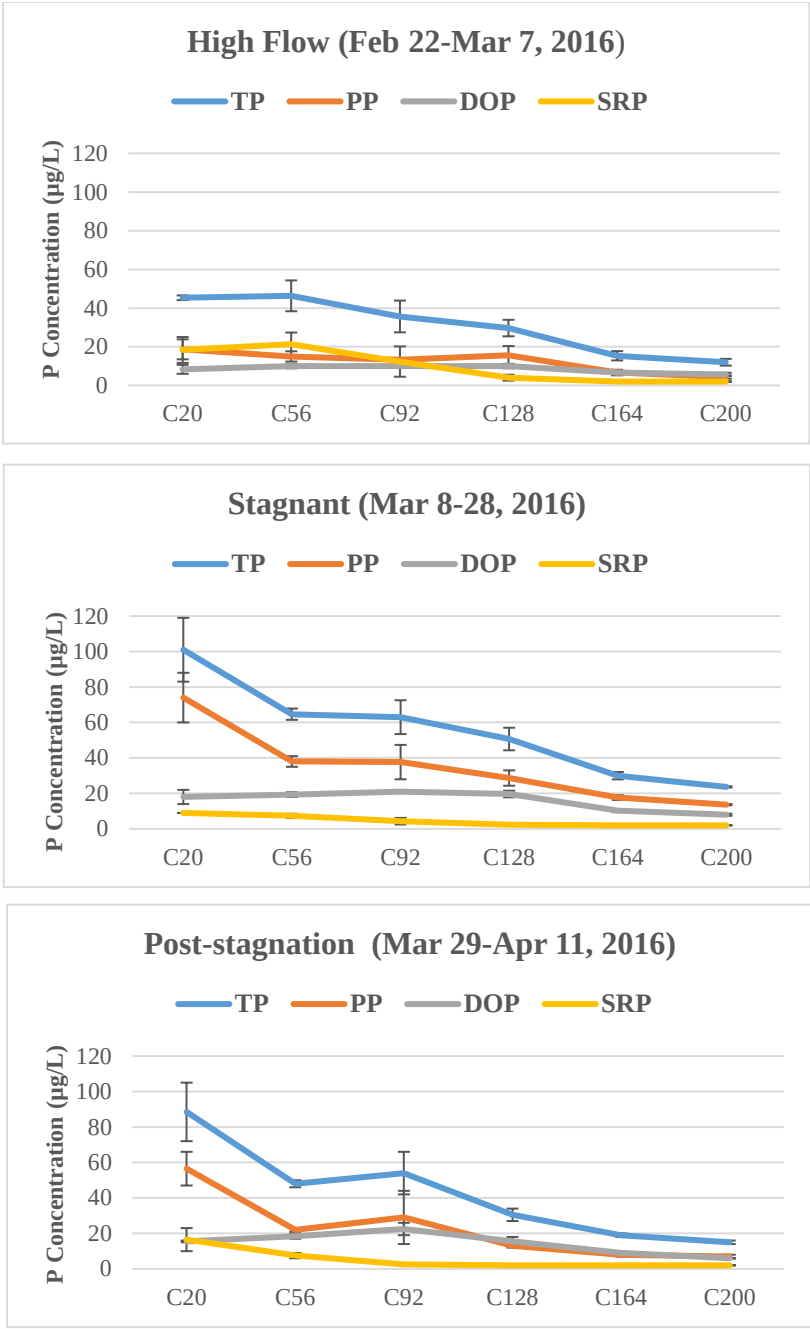

Figure 13. Water column P forms and concentrations along the transect during the flow event. Error bars represent standard error of the mean.

Other Water Quality Parameters

The following analyses describe observations on spatial patterns for surface water temperature, pH, specific conductance, dissolved oxygen, chlorophyll, ammonium, nitrogen oxides (NO_x), TN, DOC, calcium, magnesium, potassium, and iron. Further data analysis and data collection would determine correlation with spatial and temporal P cycling and reduction.

Surface Water Temperature

Surface water temperatures for all stations ranged from 13.7 degrees Celsius (° C) to 33.1° C (**Figure 14**). Daily mean water temperatures did not significantly differ between stations during the entire flow event (χ^2 = 0.77, DF = 5, p = 0.98), presumably due to the relatively consistent water depths across the cell. Mixing driven by wind across a relatively open water SAV-dominated cell may have had an impact on the results.

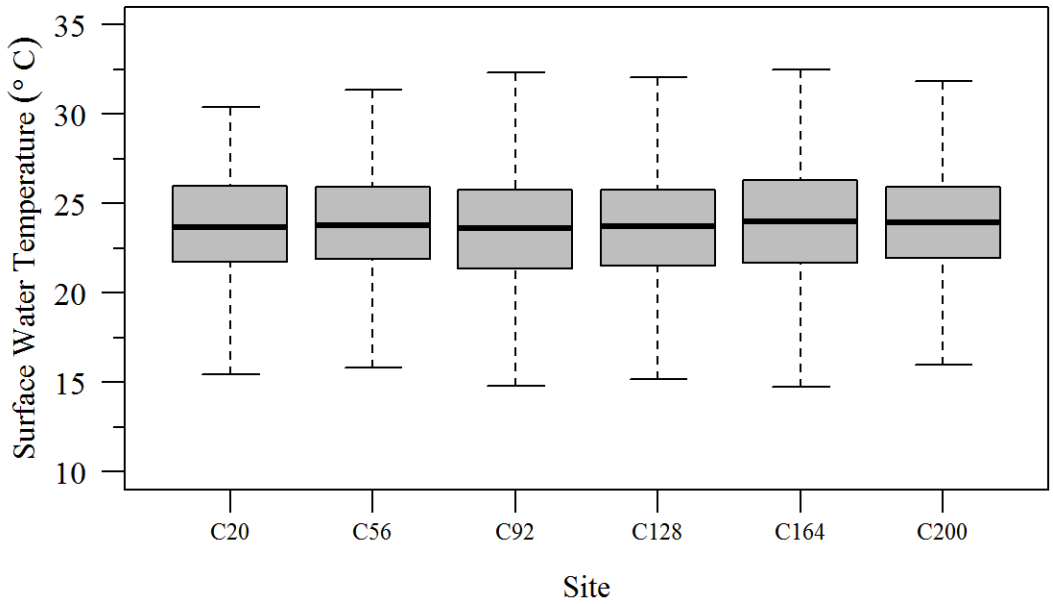

Figure 14. Boxplot of 15-minute surface water temperature data for all stations across flow periods.

Surface Water pH

Water pH varied widely from 7.3 to 10.4 during the flow event (**Figure 15**). Daily mean water pH significantly differed between stations (χ^2 = 28.9, DF = 5, p < 0.01) with stations in the mid-regions of the flow-way experiencing larger diel swings than stations closer to the inflow and outflow regions (**Figure 15**). Generally, surface water pH was highest at the mid-regions of the cell (Stations C92 and C128). Changes in pH between flow periods increased over time. Large differences in diel pH are common in freshwater SAV communities. Dierberg et al. (2002) reported pH values that ranged from 7.36 to 10.76 for different SAV mesocosms. Differences in pH (and dissolved oxygen) could be the result of intense SAV and periphyton photosynthesis and respiration throughout the diel cycle. Elevated pH values can lead to calcium carbonate ($CaCO_3$) supersaturation, which in turn may facilitate removal of P via co-precipitation (Dierberg et al. 2002, Reddy and DeLaune 2008). Furthermore, high pH values could cause low dissolved inorganic carbon, which acts as the primary carbon source for most photosynthetic organisms, ultimately influencing productivity and biomass turnover (Findlay et al. 2002, Bossio et al. 2006).

Figure 15. Boxplot of 15-minute surface water pH data across flow events. Mean surface water pH for any two stations with the same letter are not significantly different at α = 0.05 using Dunn's test of multiple comparisons.

Dissolved Oxygen

Dissolved oxygen concentrations exhibited large diel swings. Dissolved oxygen concentrations ranged from 0.0 to 33.6 mg/L, with significant differences between stations (**Figure 16**) (χ^2 = 12.58, DF = 5, $p < 0.05$). The highest variability in DO concentrations during this flow event occurred in the middle of the flow-way (Stations C92 and C128) while concentrations at the inflow were less variable than all other regions (**Figure 16**). Dissolved oxygen concentrations differed between flow periods for all stations. Generally, at most stations DO concentrations were slightly lower in the post-stagnant operational flow period.

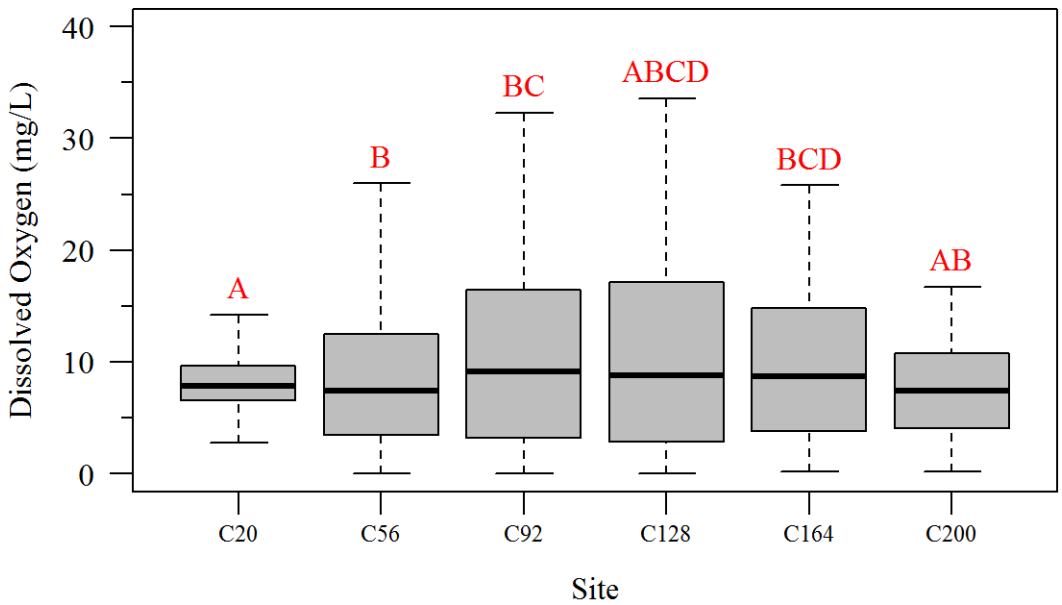

Figure 16. Boxplot of 15-minute dissolved oxygen (DO) concentrations across all flow phases. Mean DO values for any two stations with the same letter are not significantly different at α = 0.05 by Dunn's test of multiple comparisons.

Chlorophyll

Chlorophyll concentrations generally followed a diel trend with lower nighttime and higher daytime concentrations. Along the flow-way, chlorophyll concentrations were significantly different by stations (χ^2 = 173.91, DF = 5, $p < 0.01$) with concentrations being highest at the inflow (Station C20) and decreasing along the flow-way (**Figure 17**). Chlorophyll concentrations varied between flow periods for Station C20, and less for other stations along the flow-way with an average concentration of about 20 µg/L toward the end of the flow-way (**Figure 17**).

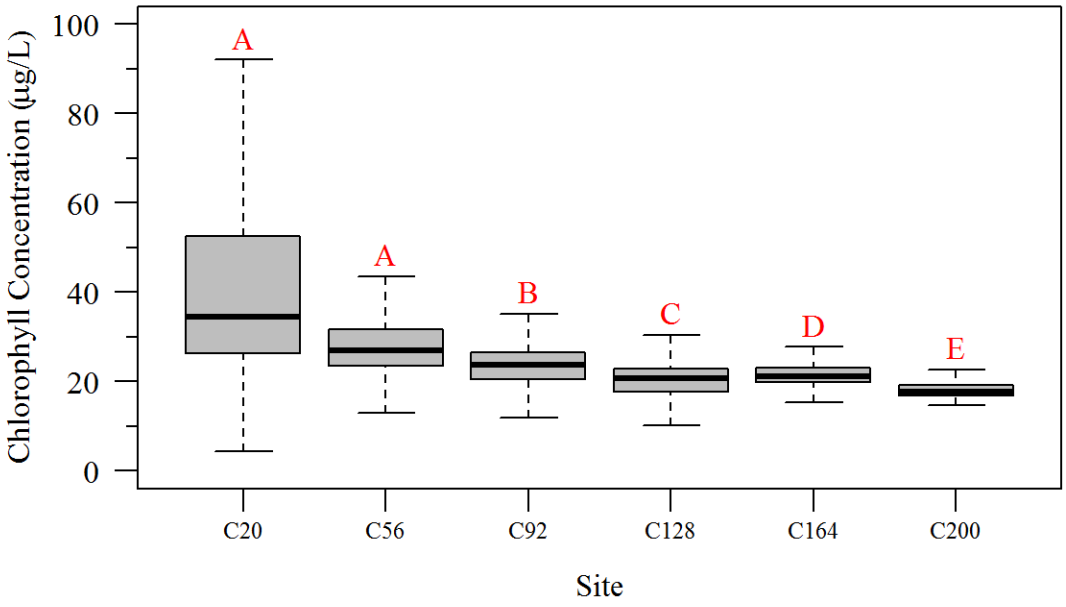

Figure 17. Boxplot of 15-minute chlorophyll data across all flow phases. Mean concentrations for any two stations with the same letter are not significantly different at α = 0.05 using Dunn's test of multiple comparisons.

Other Nutrients and Metals

TN concentrations in weekly grab samples did not change appreciably during the course of the flow test. Although TN showed a reduction of almost 17 percent, TN concentrations between inflow (Station C20) and outflow (Station C200) stations were variable (**Table 4**). Inorganic N fractions (ammonium and nitrogen oxides) were very low and accounted for less than 2 to 15 percent of TN concentrations at the different stations (**Table 4**). Ammonium mimicked TN trend but nitrogen oxides were effectively removed along the treatment flow-way, with a concentration reduction of 96 percent. DOC was fairly stable, with mean values ranging narrowly from 30 to 32 mg/L (**Table 4**). There were no noticeable changes in magnesium and potassium concentrations, but calcium and iron showed consistent reductions along the treatment flow-way during the entire flow event (**Table 4**). Mean calcium concentrations from inflow to outflow ranged from 88.9 to 61.6 mg/L, for a 31 percent reduction. Compared to calcium, mean iron concentrations were much lower and ranged from 49.3 µg/L at the inflow to 6.4 µg/L at the outflow (**Table 4**). The reduction of calcium and iron along the treatment flow-way suggests active participation of both metals in P sorption/precipitation reactions, calcium more so than iron due to a huge difference in concentrations.

Table 4. Mean concentrations of nutrients and metals in the water column along the transect during the entire flow event. Values are arithmetic averages of seven weekly grab samples.

Station	TN mg/L	NH4+ mg/L	NOX mg/L	DOC mg/L	Ca mg/L	Mg mg/L	K mg/L	Fe µg/L
C20	2.49	0.042	0.332	30.0	88.9	29.4	8.5	49.3
C56	2.26	0.034	0.207	30.7	81.1	28.6	8.4	15.6
C92	2.36	0.039	0.158	31.5	68.6	27.6	7.9	13.7
C128	2.27	0.042	0.094	32.1	63.2	27.4	8.0	11.0
C164	2.15	0.028	0.010	31.9	62.4	28.5	8.3	9.4
C200	2.07	0.041	0.013	30.9	61.6	29.7	8.3	6.4

SUMMARY

The results presented here were obtained from the flow event (two weeks of high flows, three weeks of stagnation, and two weeks of post-stagnation operational flow period with an average of 51 cfs) conducted in STA-2 Cell 3 from February 22 to April 11, 2016:

- There was a TP concentration gradient from inflow to outflow at all phases of the flow event. At the lower reaches of the treatment flow-way, TP concentrations were highest during the stagnant condition. Although TP concentrations decreased from inflow to outflow at all phases of the flow event, the spike in TP concentration at Station C92 under the stagnant and post-stagnation flow periods warrants further investigation of P release/reduction mechanisms operating within this region of the cell.
- TP in the water column was dominated by PP, followed by DOP and SRP. Reduction in TP along the flow-way was a result of reduction in all P forms. Relative to other P fractions, SRP was reduced consistently and quickly at all phases of the flow event, with outflow concentrations reaching minimum detection limit by the middle region of the flow-way at all phases of the flow event. The reduction of calcium along the treatment flow-way may suggest co-precipitation reactions with SRP and consumption by the SAV. There was a small reduction in TN concentrations along the treatment flow-way. Water pH, temperature, and dissolved oxygen demonstrated a diel pattern with low nighttime and high daytime value, and were highest at the middle region of the cell.
- Results from this flow event are preliminary. Further data analyses are underway and the results will be presented in future reports. Additional flow events are planned in this flow-way under different flow scenarios. It is anticipated that this event and a series of flow events to be conducted over the next four years at different flow-ways will provide critical information that will better explain the factors and processes influencing STA performance and develop management strategies that will help the STAs achieve lower TP discharge concentrations.

PHOSPHORUS FLUX MEASUREMENTS

Mike Jerauld[3] and Tom DeBusk[3]

INTRODUCTION

This field investigation was intended to identify and quantify process-level P flux pathways in the STAs. Specifically, the objectives are to (1) measure net P flux rates along the inflow to outflow gradient of selected flow-ways, (2) isolate the relative contributions of vegetation and diffusive flux to net P flux, and (3) identify soil variables that influence P flux. The processes contributing to surface water TP concentration include interactions between the soil, water, and biota, particularly primary producers. Based on published information on P cycling in wetlands and historical data in the STAs, it has been hypothesized that there is a relationship between soil P and water column TP through direct diffusion, resuspension, and plant uptake and turnover, but this relationship has not been quantified. Also, the relative contribution of each of these processes along the inflow to outflow gradient in STA flow-ways is unknown. Although diffusion of P from porewater to surface water has been studied in many wetlands (Fisher and Reddy 2001, Dunne et al. 2010), there is evidence that sediment P-mining and turnover of aquatic macrophytes (e.g., SAV) can contribute substantially to surface water P concentrations (Juston et al. 2013). It also is possible that burrowing macroinvertebrates can contribute to the flux of soil P to the water column, but this phenomenon has not been investigated.

METHODS

Flux measurements are made using porewater equilibrators (peepers) and in situ flux chambers (5-foot diameter bottomless high-density polypropylene) (**Figure 18**). Flux chambers are installed in triplicate in vegetated and unvegetated patches at inflow, mid-flow, and outflow regions (total 18 chambers per flow-way). To date, chambers have been installed in STA-2 Cells 1 and 3. The chambers have large open windows that allow free water exchange with the surrounding marsh, so that the enclosure experiences the same effects of P loading and other forcing factors as the rest of the cell. Following controlled, prescribed flow events, panels are installed over the windows, isolating an area of the cell. The water column in the chambers is sampled serially over a 14-day incubation period. Simultaneously, duplicate peepers are installed alongside each set of chambers, and are sampled after 14 days. The change in concentration over time inside the chambers is the net flux into or out of the water column. The diffusive flux component is calculated from the vertical profile of porewater concentrations determined by the peepers.

To date, one full-scale deployment of chambers and peepers has been conducted in Cells 1 and 3 of STA-2. The results presented here were from Cell 3 following a “high-flow” event that was implemented from February 22 to March 7, 2016 (which was preceded by high flow and high loading following heavy rainfall in January and February 2016). The chambers and peepers were sampled between March 7 and March 22, 2016. Complete descriptions of the methodology, event conditions, and full results are available in a quarterly report (DBE 2016a).

[3] DB Environmental Inc. (DBE) Rockledge, FL

Figure 18. Flux chamber installed in vegetated patch in STA-2 Cell 1 (left) and porewater equilibrator ("peeper") installed in unvegetated patch in STA-2 Cell 3.

RESULTS

The flow event in STA-2 Cell 3 was opportunistically timed at the tail end of an unusual dry season hydraulic pulse to capture high flow conditions and the response of the cell. Nominally, the P flux study defines "high" flow conditions in Cell 3 as 8.5–10 cubic meters per second (m^3/s) (300–350 cfs), giving a HLR of 8–9 centimeters per day (cm/d). The actual daily average HLR was 7–10 cm/d for the two weeks of chamber sampling. The high loading preceding the sampling in the chambers likely contributed to general P enrichment of the cell, evidenced by elevated porewater P concentrations observed at inflow and mid regions during this monitoring period (**Figure 19**).

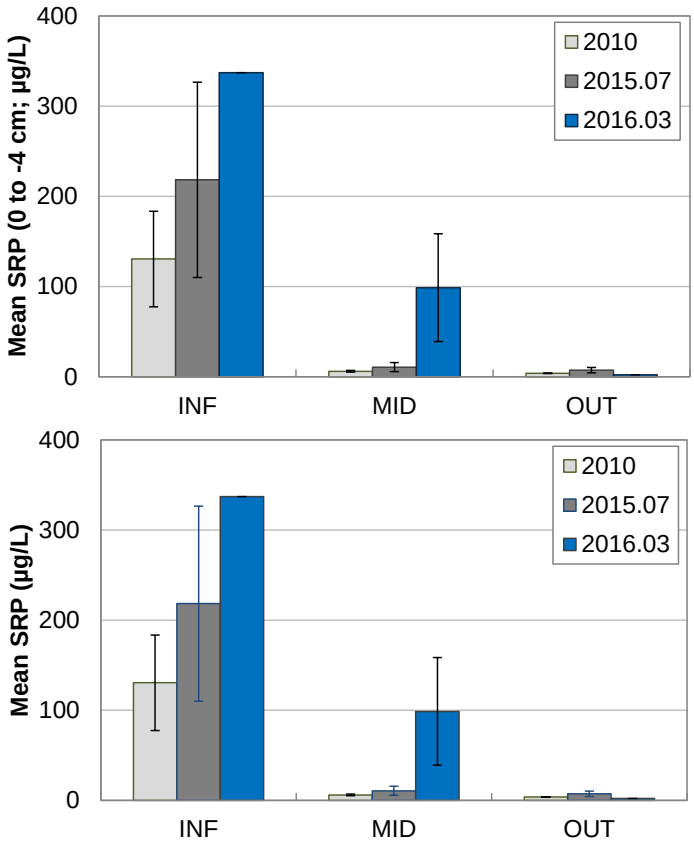

Figure 19. Mean (n = 4) porewater (0 to -4 cm) SRP concentration over time at inflow (INF), mid, and outflow (OUT) regions of STA-2 Cell 3, averaged across vegetation conditions. Error bars represent ± 1 standard error. Three of four peepers at INF were disturbed during the March 2016 deployment, so results are presented only for the single undisturbed unit.

A distinct but anticipated inflow to outflow spatial trend was evident in the concentrations of TP (**Figure 20**) and SRP (not shown) within the chambers at each measurement event. Also, TP concentrations inside the chambers increased over the 14-day period, particularly during the first 7 days, plateauing slightly thereafter, especially at mid-region and outflow stations (**Figure 21**). This indicates that, during stagnant conditions within the chambers, P was released into the water column from other sources.

At each site, the particulate fraction of TP increased over the course of the incubation. For example, in the chambers at the inflow region, PP increased from approximately 40 percent of TP on day 0 to 70 percent on day 14 (**Figure 21**). This indicates that P accumulated in the water column principally as PP, rather than soluble P fractions, as might be expected if net flux is driven mainly by diffusion. The source of that PP is not yet known, but several alternative pathways are possible, including phytoplankton uptake of SRP that may have come from the soil, senescence of SAV and attached algae (biomass turnover), and bioturbation.

Macrophytes are expected to play a significant role in net flux processes in the STAs through mining and translocation of porewater P into the water column, transpiration-driven advective flux into the soil/porewater (particularly for EAV), uptake of labile P from the water column (particularly for SAV), or combinations thereof. However, the TP response during this event generally was similar in the vegetated and unvegetated chambers (**Figure 20**). The lack of differentiation will be investigated further as additional data are collected. Vegetation effects on P flux are anticipated to be more distinct during future incubations under less P-enriched conditions.

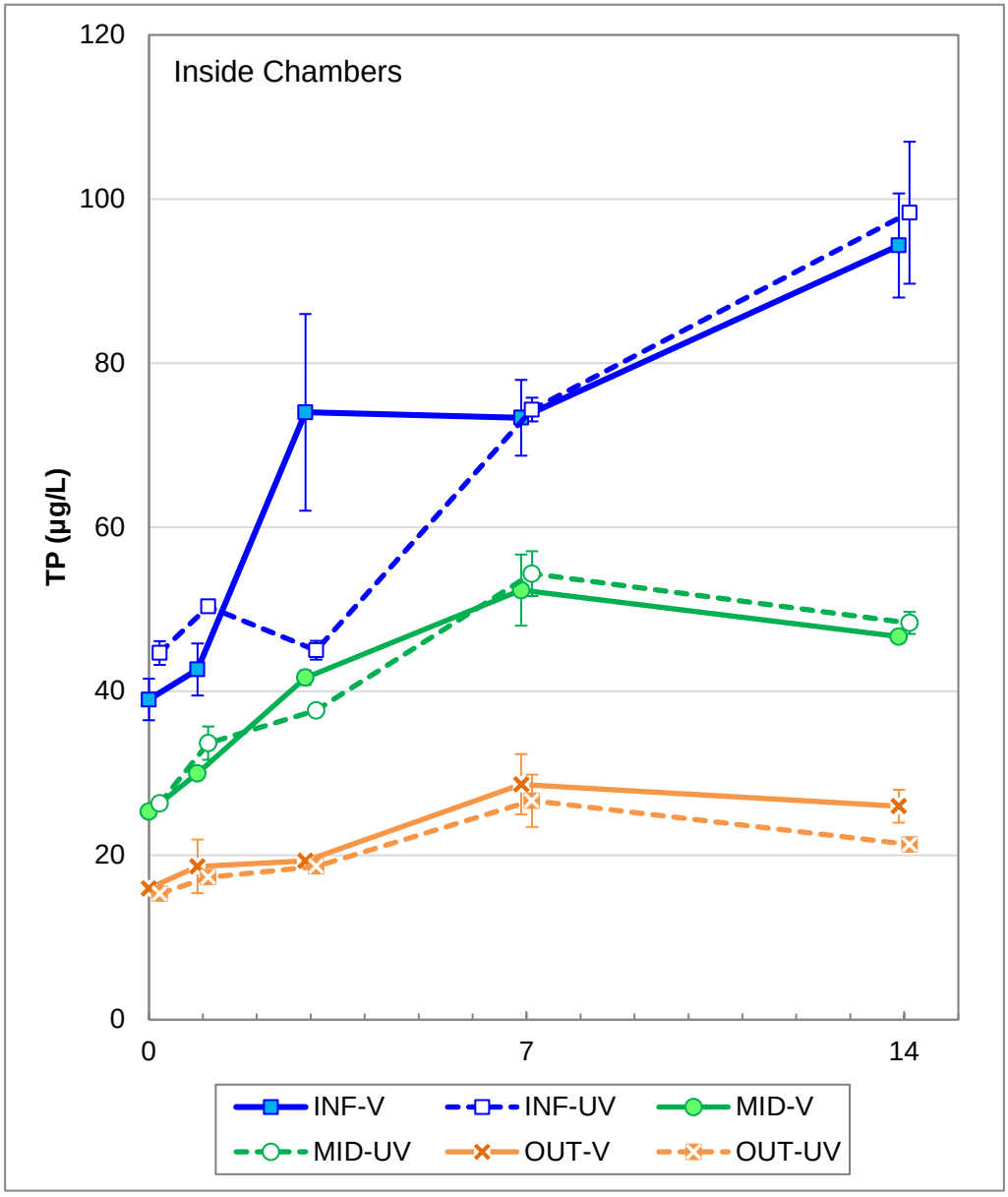

Figure 20. Average (n = 3) concentrations of TP with respect to time (days since chamber closure) in sealed flux chambers in vegetated (V) and unvegetated (UV) patches at the inflow (INF), middle (MID), and outflow (OUT) locations in STA-2 Cell 3 during March 2016. Error bars represent ± 1 standard error.

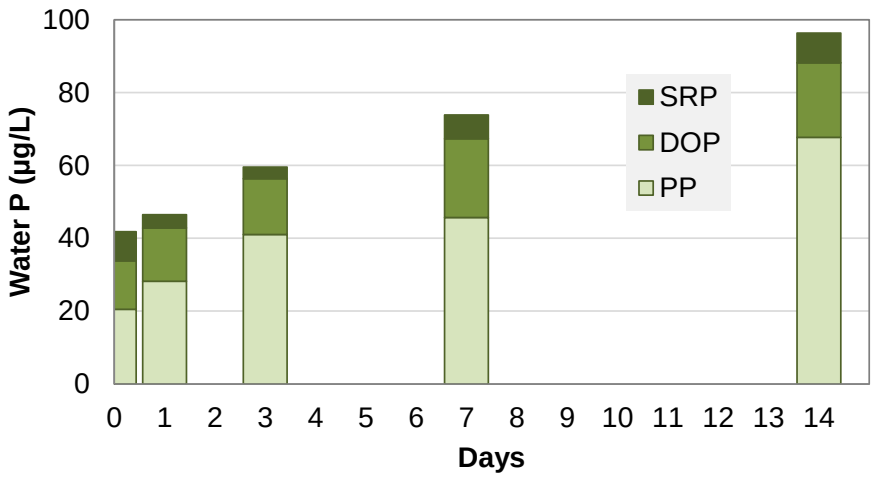

Figure 21. Average (n = 6) concentrations of SRP, DOP, and PP in surface waters of flux chambers at the inflow region of STA-2 Cell 3 during March 2016. Total bar height indicates the TP concentration, averaged between vegetation variables.

The diffusive flux rates estimated from the porewater P gradients ranged from 0.55 milligrams per square meter per day (mg/m^2/d) to slightly less than zero along the inflow to outflow gradient (**Figure 22**). This range of values is similar to those reported for the WCA-2A enrichment gradient (0 to 0.8 mg/m^2/d) (Fisher and Reddy 2001), and near the low end of diffuse flux rates measured during the initial hydration of STA-1W (0.3 to 1.5 milligrams per square meter per year [mg/m^2/yr]) (Newman and Pietro 2001). In general, these initial results from STA-2 Cell 3 suggest that diffusive flux may be a more important mechanism in the inflow region of this cell than in the outflow region of this cell (**Figure 22**).

Likewise, 14-day average net TP flux rates decreased from inflow (approximately 2 mg/m^2/d) to outflow (0.5 mg/m^2/d) (**Figure 22**), comparable to those obtained by Fisher and Reddy (2001) along the WCA-2A enrichment gradient using benthic flux chambers.

The magnitudes of diffusive fluxes co-vary with chamber-determined net flux rates (**Figure 22**); however, net flux rates were markedly higher than apparent diffusive flux rates. Similar results were reported for WCA-2A, where Fisher and Reddy (2001) observed greater net flux rates in their benthic chambers than the diffusive flux rates estimated from peepers. The data suggest that non-diffusive fluxes generally are greater than the measured diffusive fluxes along the entire gradient. In particular, net measured P flux in the outflow area of the cell seemed to be primarily from non-diffusive fluxes (**Figure 22**). Continued investigation and more data collection are needed to further understand this mechanism and its role in overall P reduction performance of the STAs.

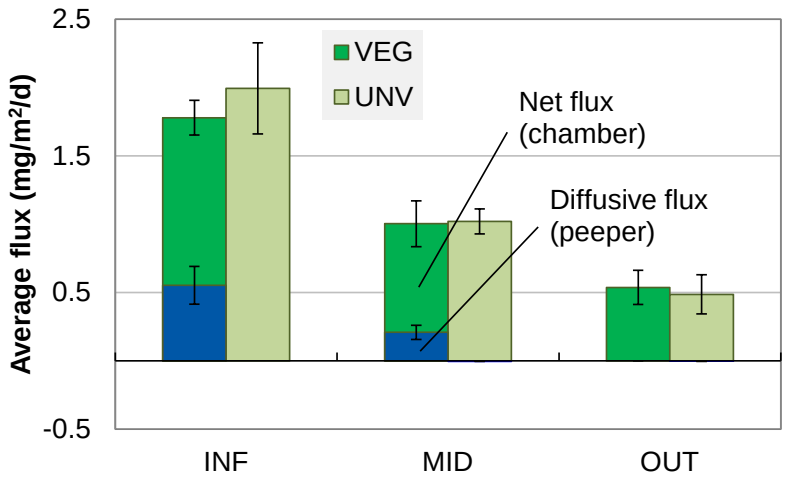

Figure 22. Mean (n = 2) TP net flux rates (green bars) calculated from flux chambers and SRP diffusive flux rates (blue bars) calculated from peepers for vegetated and unvegetated patches at each inflow (INF), middle (MID), and outflow (OUT) regions in STA-2 Cell 3 in March 2016. Error bars represent ± 1 standard error for net flux and an estimated uncertainty of ±25 percent for diffusive flux. One of the peeper units in the vegetated patch and both units in the unvegetated patch at INF were disturbed during deployment, so results are presented only for the single undisturbed unit.

SUMMARY

Initial results for porewater P concentrations and gradients suggest that the flow-way was enriched with P during this high-flow event, likely as a result of high loading in January/February 2016 that preceded the flow event. Following the cessation of flows into or out of the cell, surface water TP concentrations in the cell increased at all monitoring locations and inside the sealed flux chambers during the incubation period. This observation raises a key question that needs further investigation regarding what specific mechanisms are causing the increase of P in surface waters during stagnant conditions.

The porewater equilibrators and flux chambers detected P flux (into the water column) decreasing along a longitudinal gradient from inflow to outflow in this cell. Although chambers with macrophytes appeared to process nitrogen normally, the effects of vegetation on the P flux response were more ambiguous, perhaps as a result of the P-enriched conditions during this monitoring period. Importantly, the net fluxes measured by the chambers were substantially greater than the diffusive fluxes calculated from the peeper data at all sites, indicating contributions from non-diffusive flux mechanisms. The study will continue to focus on identifying the mechanisms responsible for this flux of P, and how those mechanisms might be manipulated.

EFFECTS OF FAUNAL COMMUNITIES ON THE WATER QUALITY IN THE EVERGLADES STORMWATER TREATMENT AREAS

Mark Cook and Joel Trexler[4]

INTRODUCTION

The influence of animals on P forms, fluxes, and transformations in the Everglades STAs has been identified as a potentially important uncertainty in their efficient management for P removal. Fauna, including waterbirds, fish, and macroinvertebrates, are increasingly recognized as important in nutrient cycling of aquatic ecosystems (Vanni 2002, Doughty et al. 2016. The abundance and mix of aquatic animals can affect water column nutrient concentration through several pathways. First, animals function as a source of internal nutrient loading by directly mobilizing benthic or particulate nutrients through feeding and excretion (Vanni et al. 2006). Second, they can have important indirect effects through modifications of the environment (e.g., bioturbation) (Vanni et al. 2006) and through top-down consumptive effects involving predator limitation of food resources and cascading interactive effects (Kellog and Dorn 2012, Dorn 2013). Bioturbation elevates water column nutrients through the resuspension of benthic nutrients and seston. Top-down effects may impact nutrient cycles if they alter the abundance of key grazers or bioturbators, altering the efficiency of animal-mediated nutrient cycles. Finally, aquatic animals can act as important P sinks and vectors of P transport (Vanni et al. 2006), especially by large mobile animals such as birds, crocodilians, and fish.

While the ecological literature points to a pivotal role of fauna in nutrient cycling, the direct and indirect roles of animals on nutrient cycles have not been studied or estimated in STAs, and their impact on P transformations are currently unknown. To gain an improved understanding of the magnitudes of these processes within the STAs, and ultimately the effect of fauna on water column total P concentrations in the STA outflow cells, the following will be provided in this substudy: (1) estimates of standing stock biomass of waterbirds (STAs 1E, 1W, and 2), fish and aquatic macroinvertebrates (STA 2), and aquatic faunal community compositional data (STAs 1E and 1W); (2) estimates of mass-specific P consumption and excretion rates of the most abundant species; and (3) experimental evaluation of the potential of benthic aquatic species to enhance water column nutrient concentrations through bioturbation. Biomass and excretion estimates will be combined to estimate areal (per hectare [ha]) P excretion by the entire faunal assemblage in STA 2 (i.e., rates of P released to the water column via excretion, micrograms of phosphorus per hectare per hour [µg P/ha/hr]). Excreted loads of P will be compared to external loads of P and the nutrient demand of SAV. Bioturbation estimates will be used to evaluate the potential of animals to alter the efficiency of benthic sequestration of total P that may be included in future P budgets and provide guidance to management actions aimed at improving P retention efficiency.

METHODS

Aquatic Fauna Sampling

Aquatic faunal sampling will be accomplished by a combination of field sampling, field experimentation, laboratory processing, and analyses. Exact procedures and sampling locations are yet to be determined but will be located within selected STA cells where other data related to the P flux study are being collected. The sampling methods (e.g., stratified or random placement) are being developed to

[4] Florida International University, Miami, FL

adequately incorporate the spatial heterogeneity in biomass of large-bodied fish and small-bodied fish/macroinvertebrates in STA outflow cells. The areal biomass (kilograms per hectare [kg/ha]) and community composition of large-bodied fish (> 4 cm standard length), small-bodied fish (< 4 cm standard length), and macroinvertebrates (e.g., crustaceans, gastropods) in STA-2 outflow cells will be estimated from throw trap surveys and electrofishing. Less intensive sampling to provide species compositional data will be gathered in STAs 1E and 1W. Mass-specific P excretion rates of the most abundant species will be estimated from a literature review and aquarium experiments. The potential for fish to re-suspend benthic nutrients will be evaluated in field mesocosm experiments.

Waterbird Surveys

Wintering populations of waterbirds of the orders Cicconiformes (storks), Pelecaniformes (herons, ibises, spoonbills), Gruiformes (rails, limpkin) and Anseriformes (ducks), were quantified using aerial video surveys. Surveys were conducted of the SAV cells in three STAs (STA-1E, STA-1W, and STA-2) on a bi-weekly basis from October through May during 2014-2015 and 2015-2016.

Aerial video surveys typically involve a special case of plot sampling called strip-transect sampling (e.g., Briggs et al. 1985), in which the camera covers long narrow strips vertically below the aircraft. Strip-transect sampling assumes that the sampled plots constitute a random sample that is representative of the entire study region, and that all individuals within a strip are detected. Thus, the number of birds counted divided by the total plot area gives an estimate of the avian density of the plot. The mean density for the plots is estimated and then applied to the entire study region.

The survey design comprised a systematic grid of parallel strip-transects oriented perpendicular to the long axis of the wetland cells (east to west) with a minimum separation distance of 500 meters (m) between successive transects. This maximized the number of transects within each STA (minimum of 20 transects per STA) to improve precision, while minimizing the likelihood that any birds disturbed during the survey were double-counted in subsequent transects. Locations of transects were determined using the survey design tool in DISTANCE 6.1 (Thomas et al. 2010), which randomly placed a grid of transect lines over the SAV cells of a given STA. The strip transects covered approximately 10 percent of the total area of the SAV cells of each STA.

Aerial surveys were conducted using a Bell 407 helicopter. A GoPro camera was attached to the pitot tube on the nose cone of the helicopter facing forward and downward at a 45° angle. Transects were flown at a speed of 60 knots and at an altitude of 30 m, which produced a video footprint 65 m in width. The three STA transects were completed in a single 3-hour flight. Flights were conducted when wind speeds were less than 30 km/h, there was no rain or fog, and visibility was more than 10 kilometers (km).

The video data are being analyzed by two trained reviewers. Double reviews are being conducted on 20 percent of the data, which was selected at random. Density estimates for each species will be analyzed using a uniform detection function in software DISTANCE (Thomas et al. 2010).

RESULTS

The aquatic fauna sampling methodology was under development in early 2016; surveys and sampling will be initiated later in the year and will proceed for two years. The results presented below are from initial assessments based on avian survey video data. While insufficient video data have been analyzed to estimate avian population sizes and densities at the scale of the STA outflow cells, a preliminary examination of the count data suggests that some groups of waterbirds can be extremely abundant and have the potential to significantly impact water quality in the treatment train. **Figure 39** shows the total number of birds, categorized into basic waterbird groups, observed from the video surveys of STA-1W and STA-2 on November 21, 2014. This survey date was selected at random and the numbers of birds are comparable to those from other survey in the STAs. Of note is the large number of American coots (*Fulica americana)* with 14,605 and 12,130 individuals for STA-1W and STA-2, respectively, which overwinter in the STAs

and feed largely on SAV. Indeed, the final estimated population sizes will be considerably greater than these counts because the surveys covered only 10 percent of the area of the SAV cells.

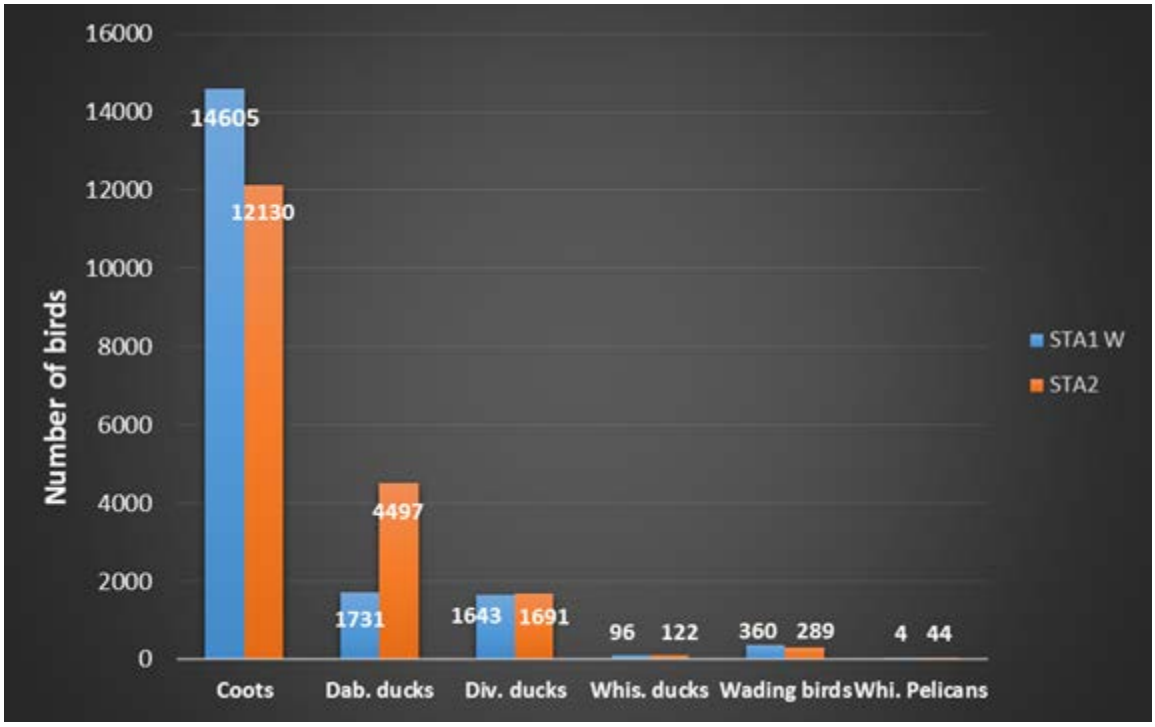

Figure 23. Numbers of waterbirds counted from aerial video surveys conducted at STAs 1W and 2 on November 21, 2014. Note that the final population estimates are expected to be considerably greater than these counts because the surveys covered only 10 percent of the area of the SAV cells.

Assuming that the average American coot consumes 90 grams of SAV (dry weight) and excretes 54 grams of guano (dry weight) per day (Kear 2005), the 14,605 birds counted in STA-1W are consuming approximately 1,315 kg SAV and producing 789 kg guano per day. Given that coot guano comprises 1.4 percent P (Kear 2005) and the population winters in the STAs for approximately six months of the year (182 days), the coots are recycling approximately 2,016 kg of TP per year. At the scale of the entire STA (STA-1W is 26,483,000 m^2), this amounts to an areal internal TP loading of approximately 0.08 $g/m^2/yr$. This loading represents 4 percent of the total external stormwater inputs of 1.9 $g/m^2/yr$ TP for this STA, and is a new contribution to the STA P budget that has not previously been addressed. While 4 percent represents only a modest contribution to TP loading, it may have a significant impact on the ability of this STA to meet the WQBEL. Moreover, four percent is a highly conservative estimate. The current count used in the calculation is based on a survey of 10 percent of the area of the SAV cells; when this is replaced by the much larger population estimate for the entire SAV cell area, and the population estimates for other waterfowl species are also included, total population estimates for STA-1W SAV cells could approach 200,000 birds. If so, the contribution to loading by waterfowl could equal that of the external loading. When interacting effects are also considered (e.g., considerable reductions in SAV cover by waterfowl consumption), it seems likely that TP concentrations in the outflow cells could be increased substantially by the presence of waterfowl. Additional data analysis and surveys are planned; results will be reported in a future SFER.

LITERATURE CITED

Bossio, D.A., J.A.Fleck, K.M.Scow and R. Fujii. 2006. Alteration of soil microbial communities and water quality in restored wetlands. *Soil Biology and Biochemistry* 38:1223-1233.

Briggs, K.T., W.B.Tyler and D.B.Lewis. 1985. Comparison of ship and aerial surveys of birds at sea. *The Journal of Wildlife Management* 49:405-411.

DBE. 2016a. *Field and Supplemental Laboratory Support for Evaluating Phosphorus Sources, Flux, and Transformation Processes in the Stormwater Treatment Areas –April 2016 Quarterly Report*. Sumbitted under Agreement 4600003029-WO01 to the South Florida Water Management District, West Palm Beach, FL.

DBE. 2016b. Field and Supplemental Laboratory *Support for Evaluating Phosphorus Sources, Flux, and Transformation Processes in the Stormwater Treatment Areas –Annual Report*. Submitted under Agreement 4600003029-WO01 to the South Florida Water Management District, West Palm Beach, FL.

Dierberg, F.E., T.A.DeBusk, S.D. Jackson, M.J. Chimney and K. Pietro. 2002. Submerged aquatic vegetation-based treatment wetlands for removing phosphorus from agricultural runoff: response to hydraulic and nutrient loading. *Water Research* 36:1409-1422.

Dorn, N.J. 2013. Consumptive effects of crayfish limit snail populations. *Freshwater Science* 32:1298-1308.

Doughty, C.E., J. Roman, S. Faurby, A. Wolf, A. Haque, E.S. Bakker, Y. Malhi, J.B. Dunning and J.C. Svenning. 2016. Global nutrient transport in a world of giants. *Proceedings of the National Academy of Sciences* 113:868-873.

Dunne, E.J., M.W. Clark, J. Mitchell, J.W. Jawitz and K.R. Reddy. 2010. Soil phosphorus flux from emergent marsh wetlands and surrounding grazed pasture uplands. *Ecological Engineering* 36(10):1392-1400.

Findlay, S.E.G., S. Dye and K.A. Kuehn. 2002. Microbial growth and nitrogen retention in litter of Phragmites australis compared to *Typha* angustifolia. *Wetlands* 22:616-625.

Fisher, M.M. and K.R. Reddy. 2001. Phosphorus flux from wetland soils affected by long-term nutrient loading. *Journal of Environmental Quality* 30(1):261-271.

Julian, P. and S. Hill. 2012. *A.R.M. Loxahatchee National Wildlife Refuge Total Phosphorus Outlier Analysis and Proposed Alternative Screening Criterion: Distribution Independent Outlier Analysis*. Presented to the Everglades Technical Oversight Committee on May 30, 2012. Available from the South Florida Water Management District, West Palm Beach, FL or online at http://www.sfwmd.gov/portal/page/portal/xrepository/sfwmd_repository_pdf/toc_tp_outlier_non-parametric.pdf.

Juston, J.M., T.A. DeBusk, K.A. Grace and S.D. Jackson. 2013. A model of phosphorus cycling to explore the role of biomass turnover in submerged aquatic vegetation wetlands for Everglades restoration. *Ecological Modelling* 251:135-149.

Kear, J. 2005. *Ducks, Geese and Swans: Species Accounts (*Cairina to Mergus*), Volume 2*. Oxford University Press, Oxford, U.K.

Kellog, C.M. and N.J. Dorn. 2012. Consumptive effects of fish reduce wetland crayfish recruitment and drive species turnover. *Oecologia* 168:1111-1121.

Newman, S. and K. Pietro. 2001. Phosphorus storage and release in response to flooding: implications for Everglades Stormwater Treatment Areas. *Ecological Engineering* 18(1):23-38.

Olsen, S.R., C.V. Cole, F.S. Watanabe and L.A. Dean. 1954. Estimation of available phosphorus in soils by extraction with sodium bicarbonate. Circular No. 939, United States Department of Agriculture, Washington, DC.

Reddy, K.R. and R.D. DeLaune. 2008. *Biogeochemistry of Wetlands: Science and Applications*. CRC Press, Boca Raton, FL.

Thomas, L., S.T. Buckland, E.A. Rexstad, J.L. Laake, S. Strindberg, S.L. Hedley, J.R. Bishop, T.A. Marques and K.P. Burnham. 2010. Distance software: Design and analysis of distance sampling surveys for estimating population size. *Journal of Applied Ecology* 47:5-14.

Vanni, M.J. 2002. Nutrient cycling by animals in freshwater ecosystems. *Annual Review of Ecology and Systematics* 33:341-370.

Vanni, M.J., A.M. Bowling, E.M. Dickman, R.S. Hale, K.A. Higgins, M.J. Horgan, L.B. Knoll, W.H. Renwick and R.A. Stein. 2006. Nutrient cycling by fish supports relatively more primary production as lake productivity increases. *Ecology* 87:1696-1709.